arXiv:1402.6087v1 [cond-mat.str-el] 25 Feb 2014

Delta chain with ferromagnetic and antiferromagnetic interactions at the critical point

V.Ya. Krivnov, D.V. Dmitriev

Joint Institute of Chemical Physics of RAS,

Kosygin str.4, 119991, Moscow, Russia.

S. Nishimoto, S.-L. Drechsler

Leibniz-Institut fuer Festkörper- und Werkstoffforschung Dresden, D-01171 Dresden, Germany

J. Richter

Institut für Theoretische Physik, Universität Magdeburg,

P.O. Box 4120, D-39016, Magdeburg, Germany

(Dated:)

We investigate the spin-1/2 Heisenberg model on the delta chain (sawtooth chain) with ferromagnetic nearest-neighbor and antiferromagnetic next-neighbor interactions. For a special ratio between these interactions there is a class of exact ground states formed by localized magnons and the ground state is macroscopically degenerate with a large residual entropy per spin $s_0 = \frac{1}{2}\ln 2$. An important feature of this model is a sharp decrease of the gaps for excited states with an increase of the number of magnons. These excitations give an essential contribution to the low-temperature thermodynamics. The behavior of the considered model is compared with that of the delta chain with both antiferromagnetic interactions.

I. INTRODUCTION

Quantum many-body systems with a single-particle flat band have attracted much attention. About twenty years ago Mielke and Tasaki [1–4] showed that a repulsive on-site interaction in flat-band Hubbard systems yields ferromagnetic ground states. More recently, a very active and still ongoing discussion of flat-band systems in the context of topological insulators has been started, see, e.g. Ref. 5 and references therein. Frustrated quantum antiferromagnets represent another active research field, where flat-band physics my lead to

interesting low-temperature phenomena [6–12], such as a macroscopic jump in the ground-state magnetization curve and a nonzero residual ground-state entropy at the saturation field as well as an extra low-temperature peak in the specific heat. All these phenomena are related to the existence of a class of exact eigenstates in a form of localized multi-magnon states which become ground states in high magnetic fields.

An interesting and typical example of such a flat-band system is the $s = \frac{1}{2}$ delta or sawtooth Heisenberg model consisting of a linear chain of triangles as shown in Fig. 1. The interaction J_1 acts between the apical (even) and the basal (odd) spins, while J_2 is the interaction between the neighbor basal sites. There is no direct exchange between apical spins. The Hamiltonian of this model has the form

$$\hat{H} = J_1 \sum (\mathbf{S}_{2n-1} \cdot \mathbf{S}_{2n} + \mathbf{S}_{2n} \cdot \mathbf{S}_{2n+1} - \frac{1}{2}) + J_2 \sum (\mathbf{S}_{2n-1} \cdot \mathbf{S}_{2n+1} - \frac{1}{4}) - h \sum S_n^z, \qquad (1)$$

where $\mathbf{S}_n$ are $s = \frac{1}{2}$ operators and h is the dimensionless magnetic field.

The ground state of model (1) with both antiferromagnetic $J_1 > 0$ and $J_2 > 0$ (AF delta chain) has been studied as a function of J_2/J_1 in Refs.13–15. At high magnetic fields for excitations above the fully polarized ferromagnetic state the lower one-magnon band is dispersionless for a special choice of the coupling constants $J_2 = J_1/2$ [16]. The excitations in this band are localized states, i.e. the excitations are restricted to a finite region of the chain. These localized one-magnon states allow to construct a set of multi-magnon states. Configurations, where the localized magnons spatially separated (isolated) from each other, become also exact eigenstates of the Hamiltonian (1). At the saturation field $h = h_s = 2J_1$ all these states have the lowest energy and the ground state is highly degenerated [9, 10, 16]. The degree of the degeneracy can be calculated by taking into account a hard-core rule forbidding the overlap of localized magnons with each other (hard-dimer rule). Exact diagonalization studies[11, 16] indicate, that the ground states in this antiferromagnetic model are separated by finite gaps from the higher-energy states. Thus the localized multi-magnon states can dominate the low-temperature thermodynamics in the vicinity of the saturation field and the thermodynamic properties can be calculated by mapping the AF delta chain onto the hard-dimer problem [9, 10, 16]. A similar structure of the ground states with localized magnons is realized in a variety of frustrated spin lattices in one, two and three dimensions such as the kagome, the checkerboard, the pyrochlore lattices, see e.g. Refs.7–12.

In contrast to the AF delta chain, the model (1) with ferromagnetic $J_1 < 0$ and antifer-

romagnetic $J_2 > 0$ interactions (F-AF delta chain) is less studied, though it is rather interesting. In particular, it is a minimal model for the description of the quasi-one-dimensional compound $[Cu(bpy)H_2O][Cu(bpy)(mal)H_2O](ClO_4)$ containing magnetic Cu^{2+} ions [23].

It is known [17] that the ground state of the F-AF delta chain is ferromagnetic for $\alpha = \frac{J_2}{|J_1|} < \frac{1}{2}$. In Ref. 17 it was argued that the ground state for $\alpha > \frac{1}{2}$ is a special ferrimagnetic state. The critical point $\alpha = \frac{1}{2}$ is the transition point between these two ground state phases.

In this paper we will demonstrate that the behavior of the model at this point is highly non-trivial. Similarly to the AF delta chain also the F-AF model at the critical point supports localized magnons which are exact eigenstates of the Hamiltonian. They are trapped in a valley between two neighboring triangles, where the occupation of neighboring valleys is forbidden (the so-called non-overlapping or isolated localized-magnon states.) We will show that the ground states in the spin sector $S = S_{\max} - k$, $k < N/4$, consist of states with k isolated localized magnons (k-magnon states), but in contrast to the AF case they are exact ground states at zero magnetic field [18]. Moreover, in addition to k-magnon configurations consisting of non-overlapping localized magnons there are states with overlapping ones. Hence, the degree of degeneracy of the ground state is even larger than in the AF delta chain. Another difference to the localized-magnon states in the AF delta chain concerns the gaps between the ground state and the excited states which become very small for $k > 1$. It means that the contribution of the ground states to the thermodynamics does not dominate even for low temperatures.

Our paper is organized as follows. In Section II we consider the ground states of the F-AF delta chain at the critical point. Based on the localized-states scenario we calculate analytically the degree of the ground-state degeneracy and check our analytical predictions by comparing them with full exact diagonalization (ED) data for finite chains up to $N = 24$ sites. In the Section III we study the low-temperature thermodynamics of the considered model. We will show that the low-lying states are separated from the ground states by very small gaps. These low-lying excitations give the dominant contribution to the thermodynamics as the temperature grows from zero and approaches these small gaps. We calculate different thermodynamic quantities, such as magnetization, susceptibility, entropy, and specific heat by full ED of finite chains and discuss the low-temperature behavior of these quantities. In Section IV we consider the magnetocaloric effect in the critical F-AF

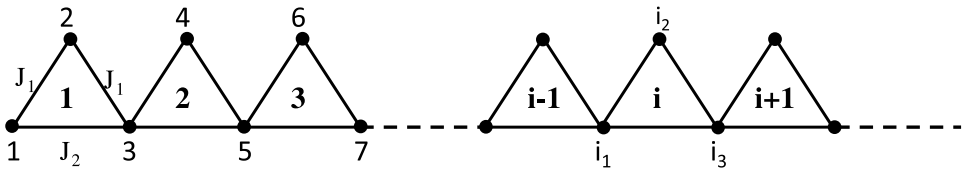

FIG. 1: The △-chain model.

delta chain. In the concluding section we give a summary of our results.

II. GROUND STATE

In this section we study the ground state of the F-AF delta chain at the critical point. For this aim it is convenient to represent the Hamiltonian (1) at $\alpha = \frac{1}{2}$ as a sum of local Hamiltonians

$$\hat{H} = \sum \hat{H}_i \tag{2}$$

where $\hat{H}_i$ is the Hamiltonian of the i-th triangle, which can be written in a form

$$\hat{H}_i = -(\mathbf{S}_{i_1} + \mathbf{S}_{i_3}) \cdot \mathbf{S}_{i_2} + \frac{1}{2}\mathbf{S}_{i_1} \cdot \mathbf{S}_{i_3} + \frac{3}{8}. \tag{3}$$

In Eq.(3) we put $J_1 = -1$. The three eigenvalues of Eq.(3) are $E_i = 0$, $E_i = 0$ and $E_i = \frac{3}{2}$ for the states with spin quantum numbers $S = \frac{3}{2}$, $S = \frac{1}{2}$ and $S = \frac{1}{2}$, correspondingly. Because the local Hamiltonians $\hat{H}_i$ generally do not commute with each other, for the lowest eigenvalue E_0 of $\hat{H}$ holds

$$E_0 \geq \sum E_i = 0. \tag{4}$$

It is evident that the energy of the ferromagnetic state with maximal total spin $S_{\max} = \frac{N}{2}$ of model (2) is zero. Therefore, the inequality in Eq.(4) turns in an equality and the ground state energy of Eq. (2) is zero. The question is: how many states with different total spin have zero energy?

At first, we consider one-magnon states with $S = S_{\max} - 1$. The spectrum $E(q)$ of these states for the F-AF delta chain with periodic boundary conditions (PBC) has two branches. One of them is dispersionless with $E(q) = 0$ while the second branch is dispersive and its energy is

$$E(q) = 2 - \sin^2 q, \quad -\frac{\pi}{2} < q < \frac{\pi}{2}. \tag{5}$$

The dispersionless one-magnon states correspond to localized states which can be chosen as

$$\hat{\varphi}_1 |F\rangle = (s_2^- + s_4^- + 2s_3^-) |F\rangle\,,\ \hat{\varphi}_2 |F\rangle = (s_4^- + s_6^- + 2s_5^-) |F\rangle\,,\ \ldots\ ,\hat{\varphi}_n |F\rangle = (s_N^- + s_2^- + 2s_1^-) |F\rangle \tag{6}$$

where $n = \frac{N}{2}$ and $|F\rangle = |\uparrow\uparrow\uparrow \ldots \uparrow\rangle$. These functions are exact eigenfunctions of each local $\hat{H}_i$ with zero energy. It can be checked directly that $\hat{H}_l \hat{\varphi}_l |F\rangle = 0$ and $\hat{H}_{l+1} \hat{\varphi}_l |F\rangle = 0$, while for other $i \neq l-1, l$ the local Hamiltonian $\hat{H}_i$ and the operators $\hat{\varphi}_l$ defined by Eq.(6) commute giving $\hat{H}_i \hat{\varphi}_l |F\rangle = \hat{\varphi}_l \hat{H}_i |F\rangle = 0$. The n states (6) form a complete nonorthogonal basis in the space of the dispersionless branch. It follows from the fact that the relation

$$\sum a_i \hat{\varphi}_i = 0 \tag{7}$$

is fulfilled if all $a_i = 0$, only. Besides, we note that there are $(n-1)$ linear combinations of $\hat{\varphi}_i |F\rangle$ which belong to the states with $S = S_{\max} - 1$ and one combination belongs to $S = S_{\max}$. The latter is

$$\sum \hat{\varphi}_i |F\rangle = 2S_{tot}^- |F\rangle\,. \tag{8}$$

For the F-AF delta chain with open boundary conditions (OBC) and odd N there are $n = \frac{N+1}{2}$ localized one-magnon states with zero energy and their wave functions are

$$\hat{\varphi}_1 |F\rangle = (s_2^- + 2s_1^-) |F\rangle\,,\ \hat{\varphi}_2 |F\rangle = (s_2^- + s_4^- + 2s_3^-) |F\rangle\,,\ \ldots\ ,\hat{\varphi}_n |F\rangle = (s_{N-1}^- + 2s_N^-) |F\rangle\,. \tag{9}$$

These functions are linearly independent similarly to those for the periodic delta chain. It is convenient to introduce another set of linearly independent operator functions instead of $\hat{\varphi}_i$ which have the form

$$\hat{\Phi}(m) = \sum_{i=1}^{m} \hat{\varphi}_i, \quad m = 1, 2 \ldots n \tag{10}$$

All functions $\hat{\Phi}(m) |F\rangle$ are eigenfunctions with zero energy of each local Hamiltonian $\hat{H}_i$. Similarly to the periodic chain the $(n-1)$ functions $\hat{\Phi}(m) |F\rangle$ with $m = 1, 2, .., n-1$ belong to $S = S_{\max} - 1$ and $\hat{\Phi}(n) |F\rangle$ is the function of the state with $S = S_{\max}$ and $S^z = S_{\max} - 1$ because $\hat{\Phi}(n) = 2S_{tot}^-$.

Let us consider two-magnon states. For simplicity we will deal with the delta chain with OBC. It is clear that the pair of isolated (non-overlapping) magnons is an exact ground state of the Hamiltonian (2) and the wave functions of pairs, $\hat{\varphi}_i \hat{\varphi}_j |F\rangle$ $(j \geq i+1)$ are exact ground state functions of each local $\hat{H}_l$ with zero energy. The number of such pairs is C_{n-1}^2,

where $C_m^n = \frac{m!}{n!(m-n)!}$ is the binomial coefficient. It can be proved similarly to the case of the AF delta chain [19] that these states are linearly independent.

In fact, the exact two-magnon ground state wave functions of the Hamiltonian (2) at $\alpha = \frac{1}{2}$ can be chosen by many other ways. We determine the set of two-magnon states as following

$$\hat{\Phi}(m_1)\hat{\Phi}(m_2)\,|F\rangle\,, \quad 1 \leq m_1 < m_2 \leq n-1. \tag{11}$$

Though Eq. (11) contains products of interpenetrating operator functions $\hat{\varphi}_i$ (i.e. acting on commonly involved sites), it is easy to be convinced that the states defined in Eq. (11) are exact ground state wave functions of each $\hat{H}_l$. For example, let us consider the function $\hat{\Phi}(1)\hat{\Phi}(2)\,|F\rangle$. It equals

$$\hat{\Phi}(1)\hat{\Phi}(2)\,|F\rangle = (\hat{\varphi}_1+\hat{\varphi}_2)\hat{\varphi}_1\,|F\rangle = (2s_1^-+2s_2^-+2s_3^-+s_4^-)\hat{\varphi}_1\,|F\rangle = (2S^-(1)+s_4^-)\hat{\varphi}_1\,|F\rangle\,, \tag{12}$$

where $S^-(1)$ is the lowering spin operator of the first triangle. Then, this function is an exact ground state function of $\hat{H}_1$, because $\hat{\varphi}_1$ creates a mixture of the states with $S = \frac{3}{2}$ and $S = \frac{1}{2}$ of $\hat{H}_1$ with zero energy. On the other hand, this function is an exact ground state function of $\hat{H}_2$, because it contains the combination $2s_3^- + s_4^-$ in the first bracket. It is also clear that the function (12) is an exact ground state function of $\hat{H}_i$ with $i \geq 3$ because $\hat{H}_i$ for these i commute with $\hat{\Phi}(1)\hat{\Phi}(2)$ and $\hat{H}_i\hat{\Phi}(1)\hat{\Phi}(2)\,|F\rangle = \hat{\Phi}(1)\hat{\Phi}(2)\hat{H}_i\,|F\rangle = 0$. A similar consideration can be extended to any function having the form (11). The function $\hat{\Phi}(m_1)\hat{\Phi}(m_2)\,|F\rangle$ contains the lowering operators $S^-(1,2\ldots m_1-1)$ and $S^-(1,2\ldots m_2-1)$ (where $S^-(1,2\ldots k)$ is the total lowering spin operator for the first k triangles). The construction of the brackets in Eq. (11) ensures the relation $\hat{H}_i\hat{\Phi}(m_1)\hat{\Phi}(m_2)\,|F\rangle = 0$ for $i \leq m_2$, while this relation for $i > m_2$ is fulfilled automatically. It easy to check that the set of functions (11) can be transformed to the set $\hat{\varphi}_i\hat{\varphi}_j\,|F\rangle$ $(j \geq i+1)$ using the condition $\hat{\Phi}(n) = 2S_{tot}^-$.

Strictly speaking we should also show that the set of the states (11) after a projection onto the states with $S_{tot} = S^z = S_{\max} - 2$ gives all linearly independent states in this spin sector. We checked this analytically for systems with $n = 5, 7$ (i.e. $N = 11, 15$) but we did not succeed with a rigorous proof of this statement.

Since the operator function $\hat{\Phi}(n)$ with $m_2 \leq n-1$ belongs to a state $\hat{\Phi}(m_1)\hat{\Phi}(n)\,|F\rangle = 2S_{tot}^-\hat{\Phi}(m_1)\,|F\rangle$ in the sector $S_{tot} = S_{\max} - 1$, it is not described by Eq. (11) by definition. The number of states described by Eq. (11) amounts C_{n-1}^2.

Now we consider the general case of the k-magnon subspace with $S_{tot} = S^z = S_{\max} - k$. It is evident that a state consisting of k isolated localized magnons

$$\hat{\varphi}_{i_1}\hat{\varphi}_{i_2}\hat{\varphi}_{i_3}\ldots\hat{\varphi}_{i_k}\left|F\right\rangle, \quad i_l > i_{l-1}+1 \tag{13}$$

is an exact ground state of Eq. (2). The number of such states is C^k_{n-k+1} and they are feasible if $k < \frac{n+1}{2}$ for OBC. However, the set of states (13) does not present the complete manifold of the ground states in the sectors of $S_{tot} = S^z = S_{\max} - k$ for $k > 2$. Similarly to the two-magnon case we choose the k-magnon set in the form

$$\hat{\Phi}(m_1)\hat{\Phi}(m_2)\hat{\Phi}(m_3)\ldots\hat{\Phi}(m_k)\left|F\right\rangle, \quad 1 \le m_1 < m_2 < m_3 < \ldots m_k \le n-1. \tag{14}$$

The functions (14) are exact ground state functions of the Hamiltonian (2). This can be proved by analogy with the two-magnon case. We assume again that after projection onto $S_{tot} = S_{\max} - k$ the set of states (14) will give a complete set of linearly independent wave functions in this sector. As follows from Eq. (14) the number of these functions is C^k_{n-1}. Again we have checked and confirmed this by full ED for finite delta chains. We note that the hypothesis about the number of degenerated ground states in the sector $S_{tot} = S^z = S_{\max} - k$ has been suggested in Ref. 20 as a guess based on numerical calculations. The number of functions in Eq. (14) is larger than the number of those given in Eq. (13). Moreover, the functions of the type described by Eq. (14) are feasible for any k. In particular, for $S_{tot} = \frac{1}{2}$ there is a single ground state function with zero energy.

In addition to Eq.(14) we can choose the sets of the ground state functions in the sectors $S^z = S_{\max} - k$ and $S > S_{\max} - k$. They have the forms

$$\begin{aligned}
&\hat{\Phi}(m_1)\hat{\Phi}(m_2)\hat{\Phi}(m_3)\ldots\hat{\Phi}(m_{k-1})\hat{\Phi}(n)\left|F\right\rangle, \quad 1 \le m_1 < m_2 < m_3 < \ldots m_{k-1} \le n-1 \\
&\hat{\Phi}(m_1)\hat{\Phi}(m_2)\hat{\Phi}(m_3)\ldots\hat{\Phi}(m_{k-2})\hat{\Phi}^2(n)\left|F\right\rangle, \quad 1 \le m_1 < m_2 < m_3 < \ldots m_{k-2} \le n-1 \\
&\qquad\qquad\qquad\qquad\qquad\qquad\qquad\qquad \ldots \\
&\hat{\Phi}(m_1)\hat{\Phi}^{k-1}(n)\left|F\right\rangle, \quad 1 \le m_1 \le n-1 \\
&\hat{\Phi}^k(n)\left|F\right\rangle \quad .
\end{aligned}$$

This set of functions represents the ground state functions with $S^z = S_{\max} - k$ but $S_{tot} = S_{\max} - k + 1$, $S_{tot} = S_{\max} - k + 2$, ..., $S_{tot} = S_{\max}$.

The total number of ground states in the sector $S^z = S_{\max} - k$ amounts

$$C^0_{n-1} + C^1_{n-1} + \ldots + C^k_{n-1}. \tag{15}$$

Let us now consider the delta chain with PBC. It is evident that the ground state in the sector $S^z = S_{\max} - k$ can be formed by k non-overlapping localized magnons

$$\hat{\varphi}_{i1}\hat{\varphi}_{i2}\hat{\varphi}_{i3}\ldots\hat{\varphi}_{ik}\left|F\right\rangle. \tag{16}$$

The number of possibilities to place k magnons on a delta chain without overlap is

$$g_n^k = \frac{n}{n-k}C_{n-k}^k, \quad n = \frac{N}{2}. \tag{17}$$

This is the number of degenerated ground states in the sector $S^z = S_{\max} - k$ built by k non-overlapping localized magnons. It corresponds to the one-dimensional classical hard-dimer problem.[10, 21] The maximum number of localized magnons for the closest possible packing is $k_{\max} = \frac{n}{2}$ and $g_n^{n/2} = 2$. Remarkably, the non-overlapping localized-magnon states (16) do not exhaust all possible ones for $k > 2$. There is another way of the ground state construction. For example, we can write the exact ground state for $k = 2$ as

$$\hat{\varphi}_i(\hat{\varphi}_{i-1} + \hat{\varphi}_i + \hat{\varphi}_{i+1})\left|F\right\rangle. \tag{18}$$

Carrying out computations similarly to those for the open chain it is easy to see that the function (18) is an exact eigenfunction with zero energy for the local Hamiltonians $\hat{H}_i$, $\hat{H}_{i+1}$ and $\hat{H}_{i-1}$ and for the other ones. Formula (18) can be extended for $k > 2$ by adding corresponding brackets. On the base of the analysis of possible construction of such type we conjecture that the ground state degeneracy in the sector $S_{tot} = S^z = S_{\max} - k$ amounts

$$A_n^k = C_n^k - C_n^{k-1} + \delta_{k,n}. \tag{19}$$

According to Eq. (19) $A_n^k = 0$ for $n > k > \frac{n}{2}$ and $A_n^{n/2} = \frac{2}{2+n}C_n^{n/2}$. The third term in Eq. (19) corresponds to the special ground state for $S = 0$ described by the famous resonating-valence-bond eigenfunction [22] which is not of "multi-magnon" nature. As follows from Eq. (19) the number of the ground states for fixed $S^z = S_{\max} - k$ is

$$\begin{aligned} B_n^k &= C_n^k, \quad 0 \le k \le \frac{n}{2} \\ B_n^k &= C_n^{n/2} + \delta_{k,n}, \quad \frac{n}{2} < k \le n. \end{aligned} \tag{20}$$

Eqs.(19) and (20) have been confirmed by ED calculations of finite chains up to $N = 24$.

The total number of degenerate ground states is

$$W = 2\sum_{k=0}^{n-1} B_n^k + B_n^n = 2^n + nC_n^{n/2} + 1. \tag{21}$$

The value of the entropy per site is $s_0 = \ln(W)/N$. That is the residual entropy per site at zero magnetic field which becomes for $N \to \infty$

$$s_0 = \frac{1}{2} \ln 2. \tag{22}$$

Obviously, the residual entropy of the considered N-site interacting spin-1/2 system corresponds to the entropy of $\frac{N}{2}$ non-interacting $s = 1/2$ spins. It is interesting to compare the residual entropy of the F-AF delta chain at the critical point with that for the AF delta chain at the saturation field. For the AF delta chain it amounts $s_0^{AF} = 0.347 \ln 2$ [9, 10, 16]. i.e. s_0 is larger than s_{AF} due to the existence of the additional ground states which do not belong to the class of non-overlapping localized magnons. Concluding this section we point out that the considered model is one more example of a quantum many-body system with a macroscopic ground-state degeneracy resulting therefore in a residual entropy.

III. LOW-TEMPERATURE THERMODYNAMICS

The next interesting question is whether the degenerate ground states are separated by a finite gap from all other eigenstates. This question is important for thermodynamic properties of the model. If a finite gap exists in all spin sectors then the low-temperature thermodynamics is determined by the contribution of the degenerate ground states. Such a situation takes place for the delta chain with antiferromagnetic interactions. As it will be demonstrated below it is not the case for the considered model.

As follows from Eq.(5) the gap ΔE in the one-magnon sector is $\Delta E = 1$ (in $|J_1|$ units). However, the minimal energy of two-magnon excitations dramatically decreases. Numerical calculations show that it equals $\Delta E \approx 0.022$. The exact wave function of this state has the form

$$\begin{aligned}
\Psi \;=\; & 0.484 \sum_n (-1)^n s^-_{2n}(s^-_{2n-1} + s^-_{2n+1}) \,|F\rangle \\
& -0.321 \sum_n \sum_{m=0} (-1)^n \exp(-\lambda m) s^-_{2n}(s^-_{2n-2m-3} + s^-_{2n+2m+3}) \,|F\rangle \\
& +0.545 \sum_n \sum_{m=1} (-1)^n \exp\{-\lambda(m-1)\} s^-_{2n+1} s^-_{2n+4m-1} \,|F\rangle \\
& -0.157 \sum_n \sum_{m=0} (-1)^n \exp(-\lambda m) s^-_{2n} s^-_{2n+4m} \,|F\rangle \,,
\end{aligned} \tag{23}$$

where $\lambda \simeq 3.494$. The energy of this state is $\Delta E = 0.02177676$. It could be expected that the low-lying excited two-magnon states are formed by scattering states of magnons from the

TABLE I: Excitation gaps in the k-magnon sectors (i.e. $S_z = N/2-k$) calculated for $N = 16, 20, 24$.

	$N = 16$	$N = 20$	$N = 24$
$k = 1$	1.0	1.0	1.0
$k = 2$	0.021776237324972	0.021776745369208	0.021776760796279
$k = 3$	0.000471848035563	0.000484876324415	0.000487488767250
$k = 4$	0.000009935109570	0.000013213815119	0.000014315249351
$k = 5$	0.000003034124289	0.000000197371592	0.000000295115215
$k = 6$	0.000002583642491	0.000000064146143	0.000000004288885

dispersionless one-magnon branch. However, the wave function (23) has a more complicated specific form of a bound state.

The gaps for the k-magnon states with $k > 2$ decrease rapidly with increasing k as it can be seen from the Table 1, where the gaps in the sector $S = S_{\max} - k$ for chains with $N = 16, 20, 24$ are presented. Obviously, the gaps become extremely small.

These data clearly testify that the contribution of the excited states to the partition function cannot be neglected even for very low temperatures. Nevertheless, to clarify this point it is proper to calculate the contribution to the partition function from only the degenerate ground states. Using Eq. (20) we obtain the partition function Z of the model in the magnetic field in a form (we use PBC for the calculation since Z for the chains with PBC and OBC coincide in the thermodynamic limit)

$$Z = 2\sum_{k=0}^{n/2} C_n^k \cosh\left[\frac{(n-k)h}{T}\right] + 2C_n^{n/2}\sum_{k=0}^{n/2}\cosh\left[\frac{(\frac{n}{2}-k)h}{T}\right] - 2C_n^{n/2}\cosh\left(\frac{nh}{2T}\right) - C_n^{n/2}. \quad (24)$$

The magnetization is given by

$$M = \langle S^z\rangle = T\frac{d\ln Z}{dh}. \quad (25)$$

It follows from Eqs. (24) and (25) that M is a function of the universal variable $x = h/T$. The dependence $M(x)$ is shown in Fig. 2 for different N. As it is seen from Fig. 2 for small x the magnetization grows with the increase of N. Analyzing the magnetization curve $M(x)$ for small x one needs to distinguish the limits $x \ll 1/N$ and $x \gg 1/N$. Using Eqs. (24) and (25) we obtain the magnetization for $x \ll 1/N$ in the form

$$M = c_N\frac{N^2h}{T}, \quad c_N = \frac{2^{n-2}n(n+1) + C_n^{n/2}(\frac{3}{4}n^2 + \frac{1}{2}C_n^3)}{n^2 2^{n+2} + 4n^3 C_n^{n/2}}. \quad (26)$$

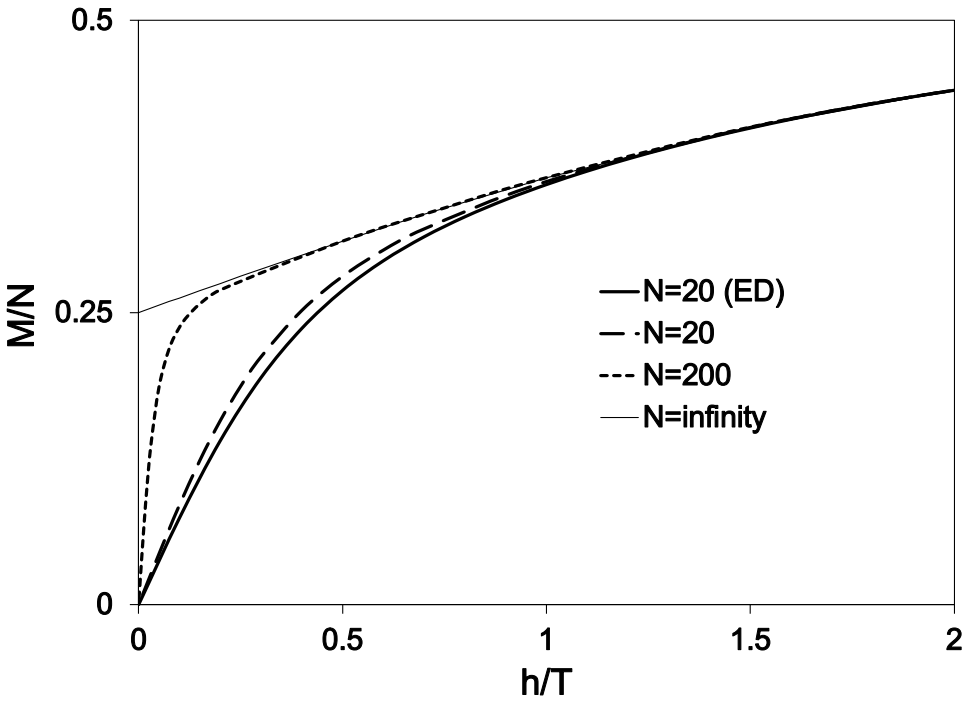

FIG. 2: Magnetization curves calculated using Eqs. (24) and (25) for $N = 20$ (long-dashed line), $N = 200$ (short-dashed line) and using Eq.(28) for $N \to \infty$ (thin solid line). Thick solid line corresponds to ED for $N = 20$ and $T = 10^{-6}$.

For $N \gg 1$, $c_N \sim 1/48$ and the magnetization per site becomes

$$\frac{M}{N} \simeq \frac{Nh}{48T}(1 + 2\sqrt{\frac{\pi}{N}}), \quad h \ll T/N. \tag{27}$$

In the opposite limit $x \gg 1/N$, the magnetization is

$$\frac{M}{N} \simeq \frac{1}{2(1 + e^{-h/T})}, \quad h \gg T/N. \tag{28}$$

However, it is clear that both equations (27) and (28) do not give an adequate description of the magnetization at $x \to 0$. For $x \ll 1/N$, M is proportional to N^2 instead of to N. On the other hand, according to Eq. (28), the magnetization in the thermodynamic limit is finite at $h = 0$. This is an artefact because the long range order (the magnetization) in one-dimensional systems can not exist at $T > 0$. Therefore, the contribution of only the degenerate ground states is not sufficient to describe the correct dependence of $M(x)$ for small x and it is necessary to take into account the contributions of other low-lying eigenstates. Unfortunately, analytical calculation of the corresponding contributions is impossible. Therefore, we carried out the full ED for $N = 16$ and $N = 20$.

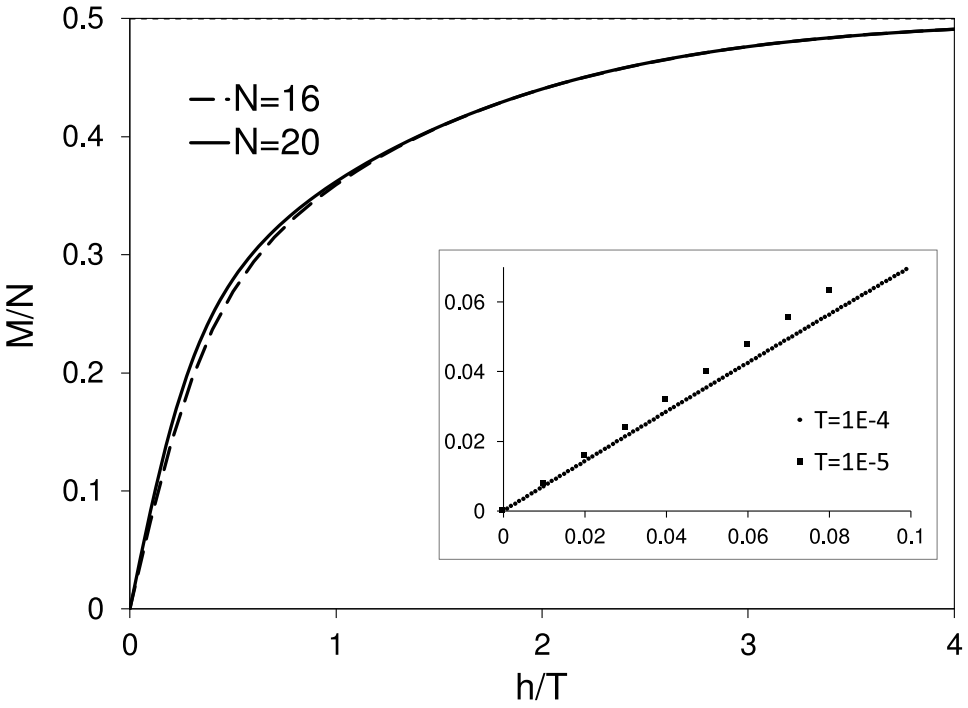

FIG. 3: Magnetization curves calculated by ED for $N = 16$ and $N = 20$ at fixed temperature $T = 10^{-6}$. The inset shows low-field limit of the magnetization curve calculated for $N = 20$ and two temperatures $T = 10^{-4}$ and $T = 10^{-5}$.

The magnetization curves obtained by ED calculations are shown in Fig. 3. It is seen that curves for $N = 16$ and $N = 20$ are close (especially at $h/T > 1$) that testifies small finite-size effects. One of the most interesting points related to the magnetization curve is its behavior at low magnetic fields. At first, we note that M obtained by ED calculations is not a function of only $x = h/T$ in contrast with the predictions given by Eqs. (27), (28). That can be seen in the inset in Fig. 3, where the magnetization for $N = 20$ is presented as a function of x for two temperatures, $T = 10^{-4}$ and $T = 10^{-5}$, i.e. in fact, $M = M(x, T)$.

In order to study the low-field limit of the magnetization curve we have calculated the uniform susceptibility per site

$$\chi = \frac{1}{3NT} \sum_{ij} \langle \mathbf{S}_i \cdot \mathbf{S}_j \rangle \,. \tag{29}$$

The calculated dependencies of $\chi(T)$ for $N = 16$ and $N = 20$ are shown in Fig. 4. For convenience they are plotted as $\ln(\chi T)$ vs. $\ln T$. Both curves are almost indistinguishable for $T > 10^{-3}$, indicating a weak finite-size dependence. A linear fit in this temperature

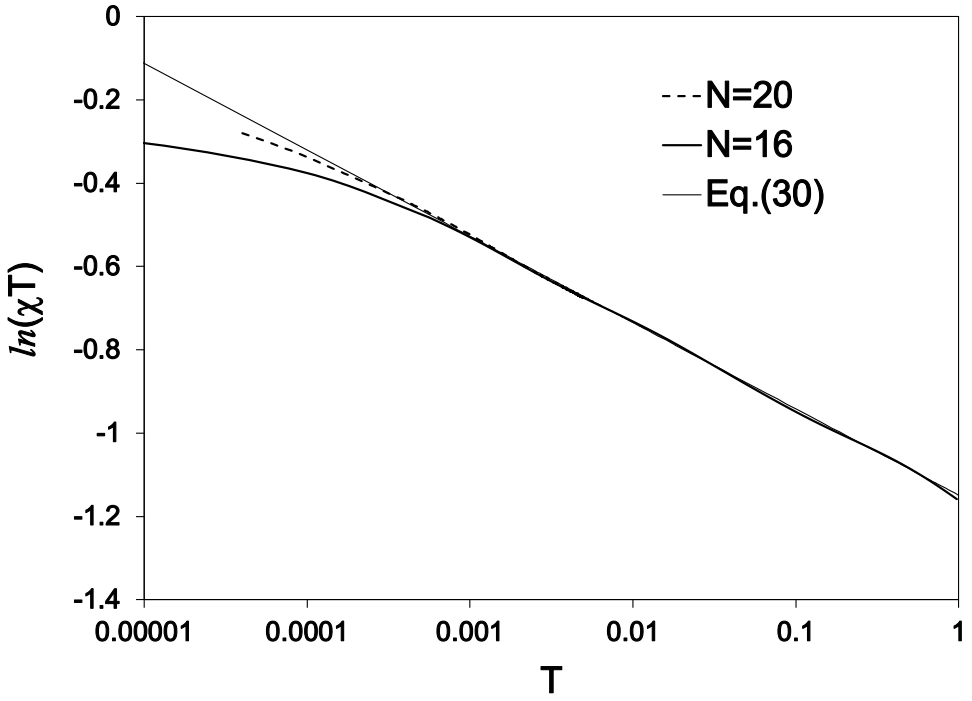

FIG. 4: Log-log plot for the dependence of the susceptibility per site on temperature calculated for $N = 16$ and $N = 20$. The thin solid line corresponds to Eq. (30).

range for the log-log plot of $\chi(T)$ yields a power-law dependence

$$\chi = \frac{c_\chi}{T^\alpha} \tag{30}$$

with

$$\begin{aligned} c_\chi &\simeq 0.317 \\ \alpha &\simeq 1.09 \end{aligned} \tag{31}$$

As shown in Fig. 4, Eq. (30) perfectly coincides with the numerical data for $N = 16$ and $N = 20$ from $T \sim 10^{-3}$ up to $T = 1$, only slight deviations near $T = 0.1$ and $T = 1$ are observed. However, for $T < 10^{-3}$ the curves $\chi(T)$ for $N = 16$ and $N = 20$ start to split and both deviate from Eq. (30).

At $T \to 0$ the susceptibility is determined by the contribution of the degenerate ground states and it is

$$\chi = c_N \frac{N}{T}. \tag{32}$$

with c_N given by Eq.(26). For $N \gg 1$ it reduces to $\chi = N/48T$.

We assume that both expressions for the susceptibility (30) and (32) are described by a single universal finite-size scaling function. This guess leads to the following form for the finite-size susceptibility:

$$\chi_N(T) = T^{-\alpha} f(c_N N T^{\alpha-1}) \tag{33}$$

Really, the behavior of the scaling function $f(z) = z$ for $z \ll 1$ provides the correct limit to Eq. (32). In the thermodynamic limit when $z = c_N N T^{\alpha-1} \to \infty$ the scaling function $f(z)$ tends to a finite value c_χ in full accord with Eq. (30). The crossover between the two types of the susceptibility behavior occurs at $z \sim 1$, which defines the effective temperature of the crossover $T_0 \sim N^{-1/(\alpha-1)}$. At $T < T_0$ the susceptibility is determined mainly by the contribution of the degenerate ground states, but this regime vanishes in the thermodynamic limit where $T_0 = 0$. Substituting the value $\alpha \simeq 1.09$ we obtain a very large exponent $\simeq 11$ for $T_0 \sim 1/N^{11}$. This exponent defines the energy scale of the excited states which contribute to the susceptibility.

The scaling hypothesis written in Eq. (33) is confirmed numerically. In Fig. 5 the ED data for $N = 16$ and $N = 20$ are plotted in the axes $\chi_N T^\alpha$ vs. $c_N N T^{\alpha-1}$. As shown in Fig. 5 the data for $N = 16$ and $N = 20$ lie very close and define the scaling function $f(z)$.

The obtained temperature dependence $\chi(T)$ (30) allows us to determine the low-field behavior of the magnetization curve

$$\frac{M}{N} = c_\chi \frac{h}{T^\alpha}. \tag{34}$$

This implies that the low field magnetization is a function of a single scaling variable $y = h/T^\alpha$. This statement is confirmed by numerical calculations, presented in Fig. 6. As shown in Fig. 6 the magnetization calculated for different (and small) values of the field h and the temperature T lies on one line when it is plotted against the scaling variable $y = h/T^\alpha$ with $\alpha = 1.09$.

The temperature dependence of the spin correlation functions $\langle \mathbf{S}_i \cdot \mathbf{S}_i \rangle$ for $N = 16$ is presented in Fig. 7. For low temperature up to $T \leq 10^{-3}$ the spin correlation functions are almost constants and the sum in Eq. (29) at $T = 10^{-9}$ is equal to c_{16} with c_{16} given by Eq. (26). For $T > 10^{-3}$ the correlations decay with the increase of T and with the distance between the spins.

Let us consider now the entropy and the specific heat. We note that the partition function

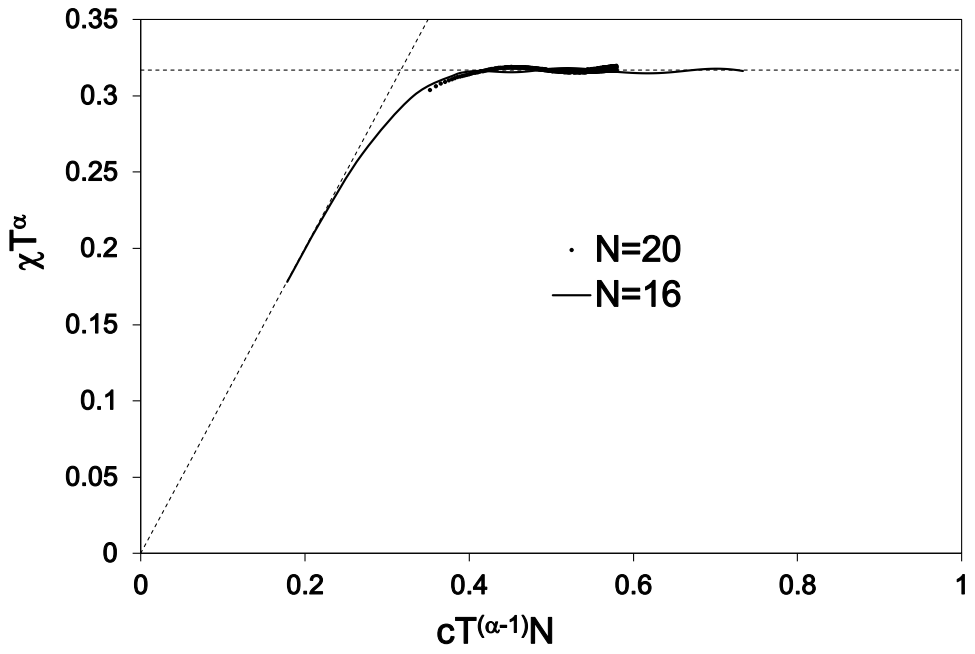

FIG. 5: Universal scaling function for the dependence of the finite-size susceptibility on temperature defined in Eq.(33) calculated by ED for $N = 16$ and $N = 20$. Thin dashed lines correspond to Eqs. (30) and (32).

(24) at $h = 0$ does not depend on the temperature, and the Helmholtz free energy is

$$\frac{F}{N} = -T \ln Z = -TS_0 \tag{35}$$

The fact that Z in Eq. (24) does not depend on T at $h = 0$ means that the partition function (24) is not relevant at $T > 0$. Nevertheless, Eq. (24) gives the exact value for the residual entropy given by Eqs. (21) and (22).

The numerical data for the T-dependence of the entropy at $h = 0$ obtained by ED are shown in Fig. 8. As it is there, the data for $N = 16$ and $N = 20$ perfectly coincide for $T > 10^{-3}$ and split for $T < 10^{-3}$. At $T \to 0$ the entropy for $N = 16$ and $N = 20$ tends to different values of the residual value given by Eq. (21). From these facts we conclude that the finite-size effects in our calculations become substantial for $T < 10^{-3}$, but the obtained data for $T > 10^{-3}$ perfectly describes the behavior of the entropy at $N \to \infty$. Therefore, we used the data for $T > 10^{-3}$ only, and found that the behavior of the entropy in the thermodynamic limit is to first approximation reasonably well described by a power-law dependence (see Fig.8):

$$\frac{S(T)}{N} = \frac{1}{2} \ln 2 + c_s T^{\lambda} \tag{36}$$

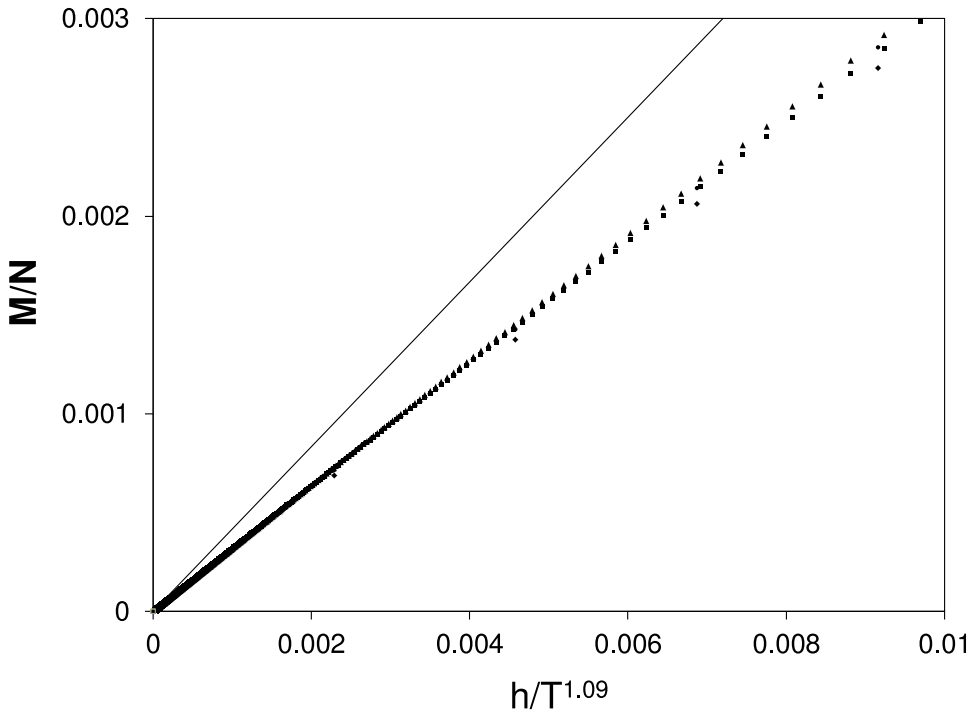

FIG. 6: Dependence of the magnetization per site on the scaling parameter $y = h/T^{1.09}$ calculated by ED ($N = 20$) for different values of the magnetic field h and temperature T. Thin solid line corresponds to Eq. (34).

with $c_s \simeq 0.245$ and $\lambda \simeq 0.12$.

The dependence of the specific heat on the temperature is presented in Fig. 9. It has a peculiar form and is characterized by a broad maximum at $T \simeq 0.7$ and two weak maxima at $T \leq 0.1$.

It is important to note that the data for $N = 16$ and $N = 20$ are slightly different at $T < 10^{-3}$ but they are indistinguishable for $T > 10^{-3}$, testifying to these data are already close to those for the thermodynamic limit. Therefore, we conclude that the prominent feature of this dependence remains relevant at $N \to \infty$.

IV. MAGNETOCALORIC EFFECT

As it is well-known [26] that spin systems with a macroscopic degenerate ground state show an appreciable magnetocaloric effect, i.e. for the cooling of the system under an adiabatic demagnetization. The standard materials for magnetic cooling are paramagnetic salts. The geometrically frustrated quantum spin systems can be considered as alternative ma-

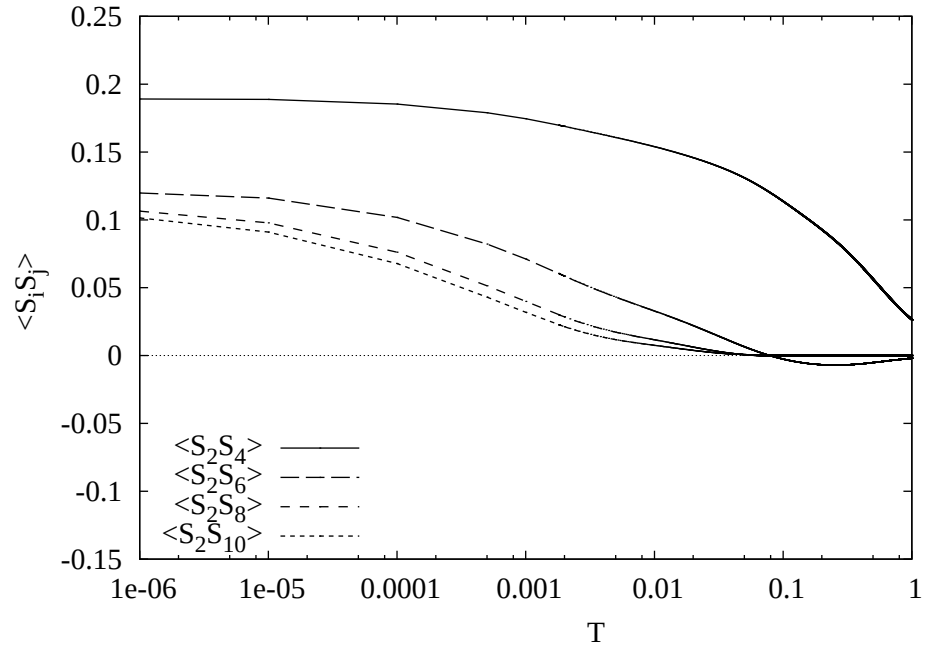

FIG. 7: Temperature dependence of various spin correlators $\langle \mathbf{S}_i \cdot \mathbf{S}_i \rangle$ (ED data for $N = 16$.) The numbering in the legend corresponds to Fig. 1 (periodic boundary conditions imposed).

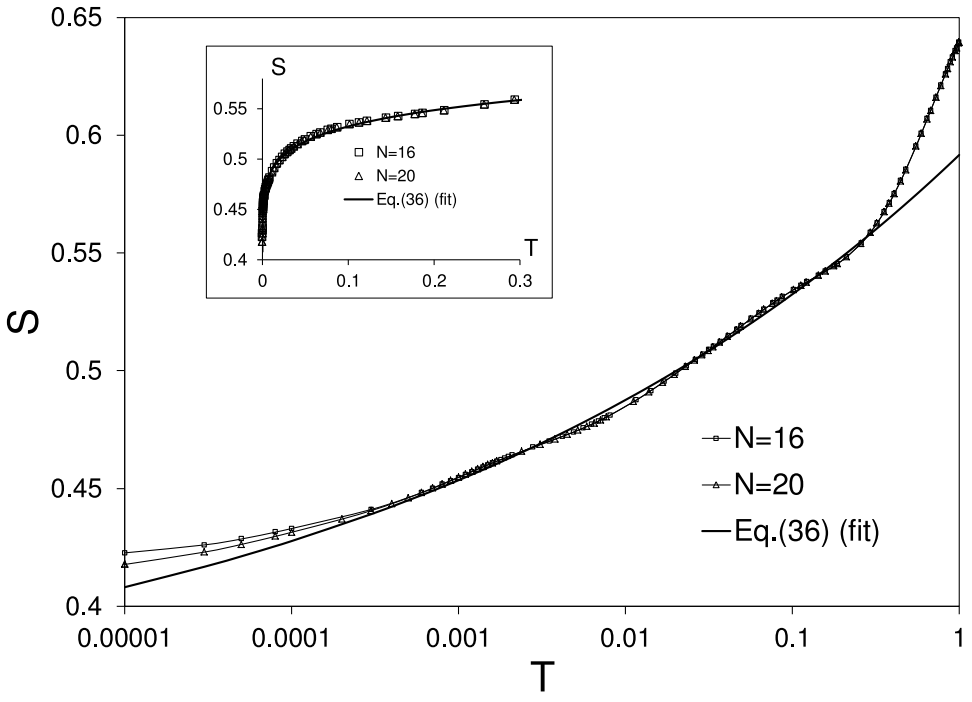

FIG. 8: Dependence of the entropy per site on temperature calculated for $N = 16$ and $N = 20$ and presented in a logarithmic scale. The thick solid line describes the approximate smooth expression given by Eq. (36). The inset shows the low-temperature limit of $S(T)$.

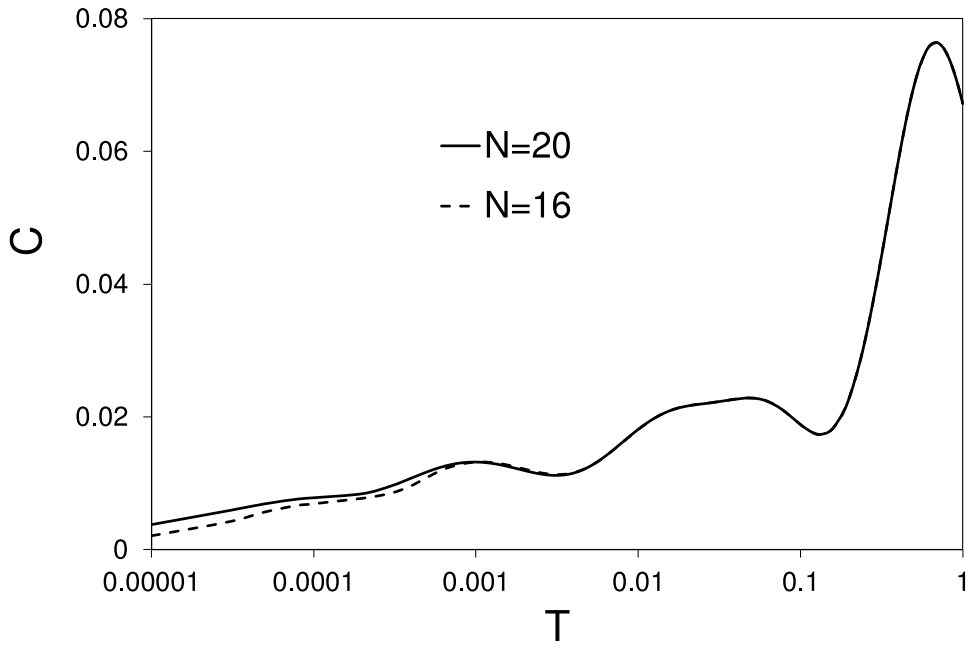

FIG. 9: Dependence of the specific heat on temperature calculated for $N = 16$ (dashed line) and $N = 20$ (solid line).

terials for low-temperature magnetic cooling. The macroscopic degeneracy of the ground state at the saturation magnetic field in some of them, including the AF delta chain, leads to an enhanced magnetocaloric effect in the vicinity of this field [11, 27–30]. However, the saturation field is relatively high in real materials and practical applications of such systems for magnetic cooling are rather questionable.

In contrast, the F-AF delta chain with $\alpha = \frac{1}{2}$ has a finite zero-temperature entropy at zero magnetic field. Therefore, it is interesting to consider the magnetocaloric properties of this model. The efficiency of the magnetic cooling is characterized by the cooling rate $(\frac{\partial T}{\partial h})_s$ and so it is determined by the dependence $T(h)$ at a fixed value of the entropy. This dependence at small h and T can be found using the results obtained in the previous Sections. According to the standard thermodynamic relations the entropy $S(T, h)$ is connected with the magnetization curve by

$$S(T,h) - S(T,0) = \frac{\partial}{\partial T} \int_0^h M(T,h')dh' \tag{37}$$

As was stated in the previous Section, there are two regions with different behavior of the magnetization curve. For very low magnetic field $h < T^\alpha$ the magnetization is proportional to h according to Eq. (34). For higher magnetic field $h > T^\alpha$ (but both $h \ll 1$ and $T \ll 1$)

the magnetization curve is described by Eq. (28). Therefore, we will consider these two cases separately.

At first we study the low-field case $h < T^{\alpha}$. Substituting the expression (34) to Eq. (37) we obtain the entropy per site $s(T,h) = S(T,h)/N$:

$$s(T,h) = s(T,0) - \frac{\alpha c_{\chi} h^2}{2T^{\alpha+1}} \tag{38}$$

where the function $s(T,0) = S(T,0)/N$ is given by Eq. (36). ¿From Eq. (38) we obtain the function $h(T)$ at constant entropy $s(T,h) = s^*$ as

$$h(T) = \sqrt{\frac{2(s_0 + c_s T^{\lambda} - s^*)}{\alpha c_{\chi}}} T^{(\alpha+1)/2} \tag{39}$$

where $s_0 = \ln 2/2$ as given by Eq. (22). From Eq. (39) we see that the cases $s^* < s_0$ and $s^* > s_0$ are different. For the case $s^* \geq s_0$ the temperature tends to the finite value T_0 at $h \to 0$:

$$T_0 = \left(\frac{s^* - s_0}{c_s}\right)^{1/\lambda}. \tag{40}$$

In other words T_0 is the lowest temperature which can be reached in the adiabatic demagnetization process if the entropy exceeds s_0. For low magnetic fields Eq. (39) allows to express the dependence $T(h)$ as:

$$T(h) = T_0 + \frac{\alpha c_{\chi} h^2}{2\lambda c_s T_0^{\alpha+\lambda}}. \tag{41}$$

In the limit $T \gg T_0$, the curve $T(h)$ transforms into

$$T(h) = \left(\frac{\alpha c_{\chi}}{2c_s}\right)^{1/(1+\alpha+\lambda)} h^{2/(1+\alpha+\lambda)}. \tag{42}$$

Substituting the values for α, c_{χ}, λ and c_s into the latter equation, we get

$$T(h) \simeq 0.85 h^{0.905} \tag{43}$$

which gives the cooling rate

$$\left(\frac{\partial T}{\partial h}\right)_{s^*} \simeq 0.77 h^{-0.095}. \tag{44}$$

As follows from Eq. (40) for the special case $s^* = s_0$ the critical temperature $T_0 = 0$ and Eqs.(43) and (44) are valid in the low temperature limit.

In the case $s^* < s_0$ we can omit the term $c_s T^\lambda$ in Eq.(39), which means that $T \to 0$ at $h \to 0$. The cooling rate for $T \ll (s_0 - s^*)^{1/\lambda}$ is given by the following expression:

$$\left(\frac{\partial T}{\partial h}\right)_{s^*} = \frac{0.413}{(s_0 - s^*)^{0.48}} h^{-0.043}. \tag{45}$$

For the case of small h and T but $h/T \gg 1$ we can calculate the integral in Eq. (37) using the expression for the magnetization given by Eq. (28). Then the entropy s^* is

$$s^* = \frac{1}{2}\ln(1 + e^{-h/T}) + \frac{h}{2T(e^{h/T} + 1)}. \tag{46}$$

This entropy coincides with the entropy per site of the ideal paramagnet of $\frac{N}{2}$ spins $\frac{1}{2}$. The transcendental Eq. (46) does not allow to derive an explicit expression for $T(h)$. However, since the magnetic field and the temperature enter Eq. (46) only in the combination h/T, the dependence $T(h)$ is a linear function. In the limit $h/T \gg 1$ ($s^* \ll 1$) one has $T(h) \sim -h/\ln(2s^*)$.

We have calculated the function $T(h)$ by ED for $N = 16$ for several fixed values of the entropy, see Fig. 10. It is seen there that the cooling rate increases when s^* approaches s_0 from below. For $s^* > s_0$ a nonzero T_0 appears, but for $T > T_0$ the cooling rate is rather high. For small h and T the behavior of the curves $T(h)$ agrees with that given by Eqs. (37)-(46).

Having in mind real materials for applications one should be aware that the expected magnetocaloric effect is expected to be somewhat reduced due to deviations from the critical point considered here and always present residual interactions beyond those considered in Eq. (1). A quantitative and systematic study of these cases is postponed to subsequent studies.

V. CONCLUSION

We have studied the ground state and the low-temperature thermodynamics of the delta chain with F and AF interactions at the transition point between the ferromagnetic and the ferrimagnetic ground states. The most spectacular feature of this frustrated quantum many-body system is the existence of a macroscopically degenerate set of ground states leading to a large residual entropy per spin of $s_0 = \frac{1}{2}\ln 2$. Remarkably, for these ground states explicit exact expressions can be found. Among the exact ground states in the spin sector

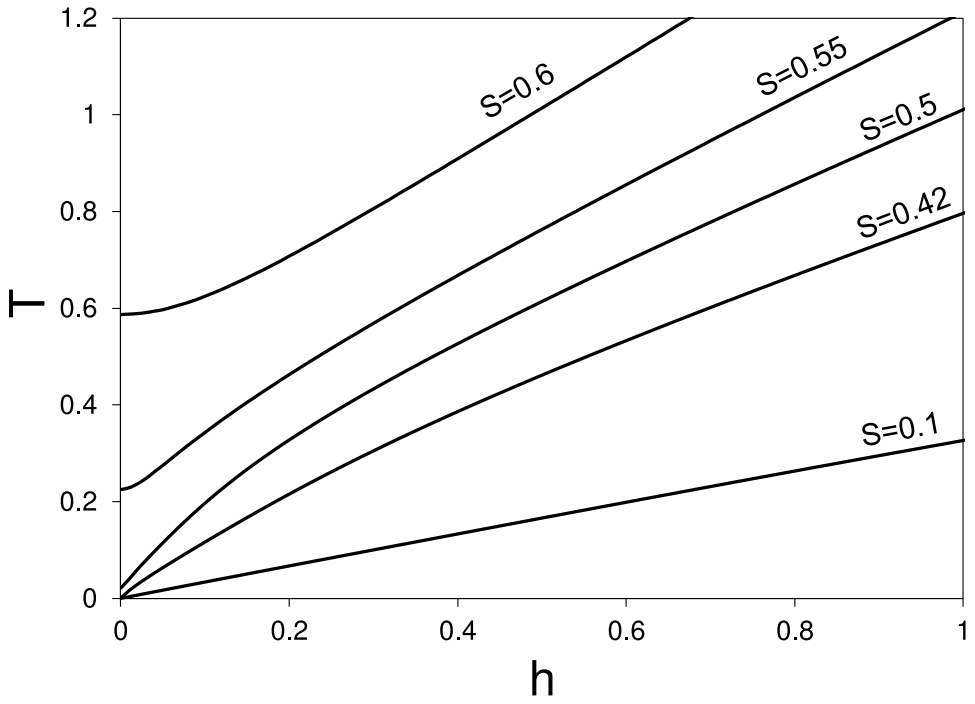

FIG. 10: Constant entropy curves as a function of the applied magnetic field and temperature for $N = 16$.

$S_{tot} = S_{\max} - k$ there are states consisting of k independent (non-overlapping) magnons each of which is localized between two neighboring apical sites. The same class of localized ground states exist for the sawtooth model (1) with both AF interactions at the saturation field [9, 10, 16]. However, such states do not exhaust all ground states in the considered model. In addition to them, there are exact ground states of another type consisting of products of overlapping localized magnons. Since such states do not exist for the sawtooth chain with both AF interactions, in this respect the considered model with F and AF interactions differs from the AF model. We have checked our analytical predictions for the degeneracy of the ground states in the sectors $S_{tot} = S_{\max} - k$ by comparing them with numerical data for finite chains. The ground-state degeneracy grows exponentially with the system size N and leads to above mentioned finite entropy per site at $T = 0$. A characteristic property of the excitation spectrum of the k-magnon states is the sharp decrease of the gap between the ground states and the excited ones when k grows. As a result both the highly degenerate ground-state manifold as well as the low-lying excited states contribute substantially to the partition function, especially at small T. That is confirmed by the comparison of the data for the magnetization M and the susceptibility χ obtained by ED of finite chains with those

given by the contribution of the only degenerate ground states. The subtle interplay of ground states and excited states leads to unconventional low-temperature properties of the model. We have shown that the magnetization M at small h and T is a function of the universal variable h/T^{α} with an index $\alpha = 1.09 \pm 0.01$. This value of α agrees with the critical index for the susceptibility. Furthermore, we have analyzed the behavior of χ for finite chains. We have found that this behavior can be described by one universal finite-size scaling function. The entropy and the specific heat have also been calculated by ED for finite chains. The entropy per site is finite at $T = 0$ and increases approximately with a power-law dependence at $T > 0$. The temperature dependence of the specific heat has a rather interesting form characterized by a broad maximum at $T \simeq 0.7$ and two weak maxima at $T \leq 0.1$.

Similar as the model with both AF interactions there is an enhanced magnetocaloric effect. While for AF model this enhanced effect is observed when passing the saturation field, we find it for the considered model when the applied magnetic field is switched off, which is obviously more suitable for a possible application.

In conclusion, we note that the structure of the ground state formed by the localized magnons is realized not only in the critical point of the spin-1/2 F-AF delta-chain but also in the s_1, s_2 chain, where s_1 and s_2 are the spins on the apical and the basal sites correspondingly. The critical point for this model is $\alpha_c = s_1/2s_2$ and the ground state in this critical point has the same degeneracy as for the $s = 1/2$ chain.

---

[1] A. Mielke, J. Phys. A **24**, L73 (1991); **24**, 3311 (1991); **25**, 4335 (1992); Phys. Lett. A **174**, 443 (1993).

[2] H. Tasaki, Phys. Rev. Lett. **69**, 1608 (1992).

[3] A. Mielke and H. Tasaki, Commun. Math. Phys. **158**, 341 (1993).

[4] M. Maksymenko, A. Honecker, R. Moessner, J. Richter, and O. Derzhko, Phys. Rev. Lett. **109**, 096404 (2012).

[5] E.J. Bergholtz and Zhao Liu, Int. J. Mod. Phys. B **27**, 1330017 (2013).

[6] J. Schnack, H.-J. Schmidt, J. Richter and J. Schulenberg, Eur. Phys. J. B **24**, 475 (2001).

[7] J. Schulenburg, A. Honecker, J. Schnack, J. Richter and H.-J. Schmidt, Phys. Rev. Lett. **88**,

167207 (2002).

[8] J. Richter, J. Schulenburg, A. Honecker, J. Schnack, and H.J. Schmidt, J. Phys.: Condens. Matter **16**, S779 (2004).

[9] M.E. Zhitomirsky and H. Tsunetsugu, Phys. Rev. B **70**, 100403(R) (2004).

[10] O. Derzhko and J. Richter, Phys. Rev. B **70**, 104415 (2004).

[11] O. Derzhko and J. Richter, Eur. Phys. J. B **52**, 23 (2006).

[12] M.E. Zhitomirsky and H. Tsunetsugu, Phys. Rev. B **75**, 224416 (2007).

[13] D. Sen, B.S. Shastry, R.E. Walsteadt and R. Cava, Phys. Rev. B **53** ,6401 (1996).

[14] T. Nakamura and K. Kubo, Phys. Rev. B **53**, 6393 (1996).

[15] S.A. Blundell and M.D. Nuner-Reguerio, Eur. Phys. J. B **31**, 453 (2003).

[16] O. Derzhko, A. Honecker and J. Richter, Phys. Rev. B **76**, 220402(R) (2007), J. Richter, O. Derzhko, A. Honecker, Int. J. Modern Phys. B **22**, 4418 (2008).

[17] T. Tonegawa and M. Kaburagi, J. Magn. Magn. Materials, **272-276**, 898 (2004).

[18] This is very advantageous from an experimental point of view with the aim to study these localized magnon states, since to study them at frequently high saturation fields exceeding 40 Tesla using pulsed fields, only, is this way circumvented.

[19] H.-J. Schmidt, J. Richter and R. Moessner, J. Phys. A **39**, 10673 (2006).

[20] H. Suzuki and K. Takano, J. Phys. Soc.Jpn. **77**, 113701 (2008).

[21] M.E. Fisher, Phys. Rev. **124,** 1664 (1961).

[22] T. Hamada, J. Kane, S. Nakagawa and Y. Natsume, J. Phys. Soc. Jpn. **57**, 1891 (1988).

[23] Y. Inagaki, Y. Narumi, K. Kindo, H. Kikuchi, T. Kamikawa, T. Kunimoto, S. Okubo, H. Ohta, T. Saito, H. Ohta, T. Saito, M. Azuma, H. Nojiri,, M. Kaburagi and T. Tonegawa, J. Phys. Soc. Jpn. **74**, 2831 (2005).

[24] D.V. Dmitriev, V.Ya. Krivnov and A.A. Ovchinnikov, Phys. Rev. B **56**, 5985 (1997).

[25] D.V. Dmitriev, V.Ya. Krivnov and A.A. Ovchinnikov, Eur. Phys. J. B **14**, 91 (2000).

[26] M.E. Zhitomirsky, Phys. Rev. B **67**, 104421 (2003).

[27] M.E. Zhitomirsky and A. Honecker, J. Stat. Mech.: Theor. Exp. P07012 (2004).

[28] M.E. Zhitomirsky and H. Tsunetsugu, Progr. Theor. Phys. Suppl. **160**, 361 (2005).

[29] J. Schnack, H.-J. Schmidt and J. Richter, Phys. Rev. B **76**, 054413 (2007).

[30] E. Garlatti, S. Carretta, J. Schnack, G. Amoretti and P. Santini, Appl. Phys. Lett. **103**, 202410 (2013).